ACI STRUCTURAL JOURNAL TECHNICAL PAPER

Title no. 101-S68

Flexural Modeling of Reinforced Concrete Walls—Model Attributes

by Kutay Orakcal, John W. Wallace, and Joel P. Conte

Predicting inelastic responses of reinforced concrete walls and wall systems requires accurate, effective, and robust modeling and analysis tools that incorporate important material characteristics and behavioral response features (that is, neutral axis migration, tension-stiffening, progressive gap closure, and nonlinear shear behavior). A research project was undertaken to investigate and to improve an effective modeling approach for the reliable prediction of the inelastic response of slender reinforced concrete (RC) walls that incorporates refined constitutive models and various response features. It was verified that the multiple-vertical-line-element model captures important response characteristics associated with cyclic behavior RC structural walls governed by flexure. The wall model adopted herein provides a flexible platform to assess the influence of material and other behavioral features in nonlinear responses. Variation of model and material parameters was investigated to identify the sensitivity of global and local model results to changes in these parameters.

Keywords: macroscopic; reinforced concrete; shearwall.

INTRODUCTION

Reinforced concrete (RC) structural walls are effective for resisting lateral loads imposed by wind or earthquakes. They provide substantial strength and stiffness as well as the deformation capacity needed to meet the demands of strong earthquake ground motions. Extensive research has been carried out to study the behavior of RC walls and frame-wall systems. A reliable prediction of the inelastic response both at the global and local levels of such structural systems under seismic loads requires the use of an analytical model that captures the hysteretic behavior as well as the interaction of the wall with other structural members.

Analytical modeling of the inelastic response of structural wall systems can be accomplished by using microscopic or macroscopic phenomenological models. Although microscopic (finite element) models can provide a refined and detailed definition of the local response, their efficiency, practicality, reliability, and robustness are questionable due to complexities involved in developing the model and interpreting the results. An effective analytical model for analysis and design of most systems should be relatively simple to implement and reasonably accurate in predicting the hysteretic response of RC wall systems.

A reliable model for practical nonlinear analysis of RC structural walls is not available in commonly used structural analysis platforms, such as DRAIN-2DX and SAP2000. Use of a single beam-column element (Fig. 1) at the wall centroidal axis is a common modeling approach. In this case, an equivalent column is used to model the properties of the wall, and girders with rigid end zones are connected to the column at each floor level. The rotations of a beam-column element occur about the centroidal axis of the wall; therefore, migration of the neutral axis along the wall cross section during loading and unloading is not accounted for. Consequently, effects including rocking of the wall and interaction with the connecting girders, both in the plane of the wall and perpendicular to the wall, may not be properly considered. Various phenomenological macroscopic models have been proposed to capture such behavioral features in predicting the inelastic response of RC structural walls. As a result of extensive studies,[1-7] the multi-component-in-parallel model (MCPM, later referred to as multiple-vertical-line-element model [MVLEM]) proposed by Vulcano, Bertero, and Colotti[1] has been shown to successfully balance the simplicity of a macroscopic model and the refinements of a microscopic model.[1] The MVLEM captures important features (for example, shifting of the neutral axis, and the effect of a fluctuating axial force on strength and stiffness), which are commonly ignored in simple models, and offers the flexibility to incorporate various material hysteretic models and important response features (for example, confinement and nonlinear shear behavior) in the analysis.

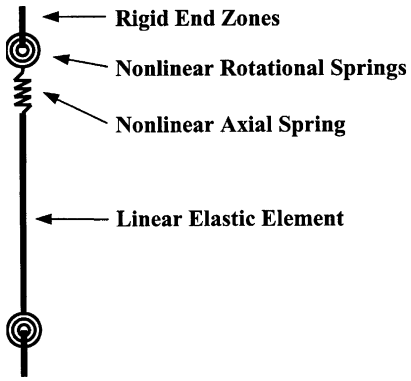

Fig. 1—Beam-column element.

Prior work identified that wall flexural response can be accurately predicted by the MVLEM when refined hysteretic constitutive laws are adopted.[1] Subsequent modifications of the MVLEM[2,3] have included implementing simplified force-deformation rules for the uniaxial elements to capture the behavior observed in experimental results; however, the resulting analytical response prediction is thus governed by somewhat arbitrary force-deformation rule parameters, the selection of which is based on engineering judgment.[2] An

ACI Structural Journal, V. 101, No. 5, September-October 2004.
MS No. 03-189 received June 3, 2003, and reviewed under Institute publication policies. Pertinent discussion including author's closure, if any, will be published in the July-August 2005 *ACI Structural Journal* if the discussion is received by March 1, 2005.

Kutay Orakcal *is a PhD student in the Department of Civil Engineering, University of California-Los Angeles (UCLA), Los Angeles, Calif. He received his BS from Middle East Technical University, Ankara, Turkey, in 1998, and his MS in civil engineering from UCLA in 2001. His research interests include behavior and modeling of reinforced concrete and steel-reinforced concrete elements and systems.*

John W. Wallace, *FACI, is an associate professor of civil engineering at UCLA. He is a member of ACI Committee 318-H, Seismic Provisions; 374, Performance-Based Seismic Design of Concrete Buildings; and Joint ACI-ASCE Committee 352, Joints and Connections in Monolithic Concrete Structures. His research interests include response and design of buildings and bridges to earthquake actions, laboratory and field testing of structural components and systems, and structural health monitoring.*

Joel P. Conte *is an associate professor of structural engineering at the University of California-San Diego, San Diego, Calif. His research interests include structural modeling, analysis, identification, and control; earthquake engineering; structural reliability; and risk analysis.*

alternative approach is adopted herein, where state-of-the-art uniaxial cyclic material constitutive laws for concrete and reinforcing steel were adopted to better predict nonlinear response at both the global and local levels.

Although extensive research has been carried out on the development of the MVLEM,[1-7] the model has not been implemented into widely available computer programs and limited information is available on the influence of material behavior on predicted responses. The model also has not been sufficiently calibrated with and validated against extensive experimental data at both local and global response levels. The reliability of the model in predicting the shear behavior of walls is questionable and an improved methodology that relates hysteretic flexural and shear responses is needed.

RESEARCH SIGNIFICANCE

Given the aforementioned shortcomings, a research project was undertaken to investigate and improve the MVLEM for slender RC wall systems, as well as to calibrate and validate it against experimental data. A description of the improved model, implementation of detailed cyclic constitutive relationships, and the sensitivity of the model predictions to both model and material parameters are presented in this paper. Detailed comparisons of model results with extensive experimental data at global and local response levels are presented in a follow-up paper. The comparisons indicate that, with proper calibration of material parameters, the model is effective in predicting the nonlinear flexural response of slender reinforced concrete walls.

ANALYTICAL MODEL

The model in Fig. 2(a) is an implementation of the generic two-dimensional MVLEM wall element. A structural wall is modeled as a stack of *m* MVLEM elements, which are placed on one another (Fig. 2(b)). The flexural response is simulated by a series of uniaxial elements (or macrofibers) connected to rigid beams at the top and bottom (for example, floor) levels. The stiffness properties and force-displacement relationships of the uniaxial elements are defined according to state-of-the-art, uniaxial, cyclic constitutive models for concrete and steel and the tributary area assigned to each uniaxial element (Fig. 3). The number of the uniaxial elements *n* can be increased to obtain a more refined description of the wall cross section.

The relative rotation between top and bottom faces of the wall element occurs around the point placed on the central axis of the element at height *ch* (Fig. 4). Rotations and resulting transverse displacements are calculated based on the wall curvature, derived from section and material properties, corresponding to the bending moment at that specific point

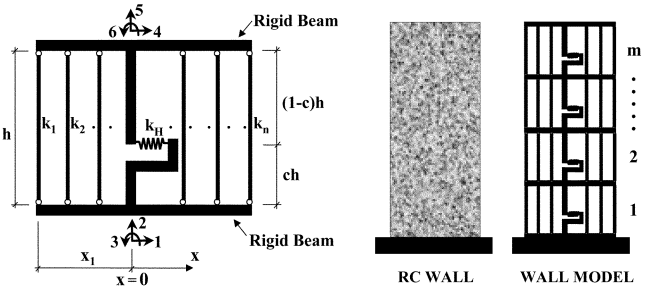

(a) MVLEM Element (b) Model of a Wall

Fig. 2—MVLEM.

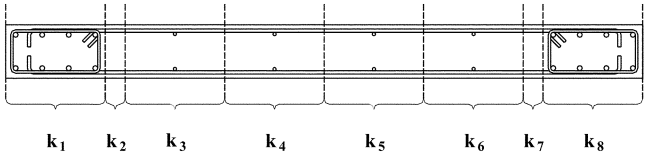

Fig. 3—Tributary area assignment.

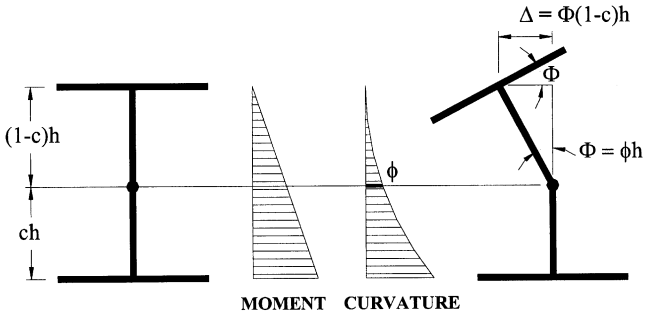

Fig. 4—Rotations and displacements of MVLEM element.

of each element (Fig. 4). A suitable value of the parameter *c* is based on the expected curvature distribution along the element height *h*. A value of $c = 0.4$ was recommended by Vulcano, Bertero, and Colotti[1] based on comparison of the model response with experimental results. Selection of *c* becomes important in the inelastic range, where small changes in moment can yield highly nonlinear distributions of curvature. Stacking more elements along the wall height, especially in the regions where inelastic deformations are expected, will result in smaller variations in the moment and curvature along the height of each element, thus improving analytical accuracy.[3]

A horizontal spring placed at the height *ch*, with a nonlinear hysteretic force-deformation behavior following an origin-oriented hysteresis model (OOHM)[4] was originally suggested by Vulcano, Bertero, and Colotti[1] to simulate the shear response of the wall element. The OOHM was proven to be unsuitable by Vulcano and Bertero[5] for an accurate idealization of the shear hysteretic behavior especially when high shear stresses are expected. The study presented herein, however, focuses on modeling and simulation of the flexural response, thus a linear elastic force-deformation behavior was adopted for the horizontal "shear" spring. Flexural and shear modes of deformation of the wall member are uncoupled (that is, inelastic flexural deformations do not affect shear strength and inelastic shear deformation), and the horizontal shear displacement at the top of the element does not depend on *c*.

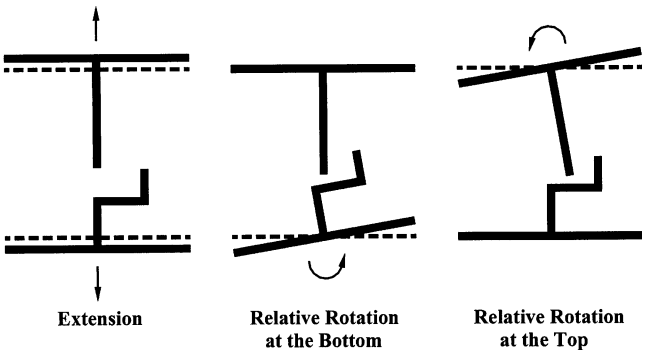

Fig. 5—Element deformations of MVLEM.

A single, two-dimensional MVLEM has six global degrees of freedom, three of each located at the center of the rigid top and bottom beams (Fig. 2(a)). According to this model, the strain level in each uniaxial element is obtained from the element six nodal degrees of freedom (translations and rotations) using the plane-sections-remain-plane kinematic assumption. Thus, if k_H is the stiffness of the horizontal spring, k_i is the stiffness of the i-th uniaxial element, and x_i is the distance of the i-th uniaxial element to the central axis of an element, the stiffness matrix of an element relative to the six degrees of freedom is obtained as

$$[K_e] = [a]^T \cdot [\mathrm{K}] \cdot [a] \tag{1}$$

where $[a]$ denotes the transformation matrix converting the element degrees of freedom to the element deformations of extension, relative rotation at the bottom, and relative rotation at the top of each wall element (Fig. 5).

$$[a] = \begin{bmatrix} 0 & -1 & 0 & 0 & 1 & 0 \\ -1/h & 0 & 1 & 1/h & 0 & 0 \\ -1/h & 0 & 0 & 1/h & 0 & 1 \end{bmatrix} \tag{2}$$

and

$$[K] = \begin{bmatrix} \sum_{i=1}^{n} k_i & -\sum_{i=1}^{n} k_i x_i & \sum_{i=1}^{n} k_i x_i \\ & k_H c^2 h^2 + \sum_{i=1}^{n} k_i x_i^2 & k_H c(1-c)h^2 - \sum_{i=1}^{n} k_i x_i^2 \\ \text{symm.} & & k_H (1-c)^2 h^2 + \sum_{i=1}^{n} k_i x_i^2 \end{bmatrix} \tag{3}$$

is the element stiffness matrix relative to the three pure deformation degrees of freedom shown in Fig. 5. Similarly, if f_H is the force in the horizontal spring, and f_i is the force in the i-th uniaxial element, the resisting force vector of the wall element relative to the six degrees of freedom is obtained from equilibrium as

$$[F] = \left[\{f_H\} \left\{ -\sum_{i=1}^{n} f_i \right\} \left\{ -f_H ch - \sum_{i=1}^{n} f_i x_i \right\} \right. \tag{4}$$

$$\left. \{-f_H\} \left\{ \sum_{i=1}^{n} f_i \right\} \left\{ -f_H (1-c)h + \sum_{i=1}^{n} f_i x_i \right\} \right]^T$$

MATERIAL CONSTITUTIVE MODELS

The stiffness and force-deformation properties of the uniaxial elements are derived from uniaxial stress-strain material behavior; therefore, various state-of-the-art uniaxial material constitutive models can be implemented. Axial models for reinforcing bar buckling and bond slip can also be incorporated into the wall model because the stiffness properties of the wall model are based on axial force-deformation relationships. Responses obtained using the present wall model were found to be sensitive to the material constitutive models used; therefore, details of the constitutive laws used in this study for steel and concrete are described in the following sections.

Uniaxial steel constitutive model

The reinforcing steel stress-strain behavior implemented in the wall model is the well-known nonlinear hysteretic model of Menegotto and Pinto,[8] as extended by Filippou, Popov, and Bertero[9] to include isotropic strain hardening effects. The relationship is in the form of curved transitions (Fig. 6(a)), each from a straight-line asymptote with slope E_0 (modulus of elasticity) to another asymptote with slope $E_1 = bE_0$ where parameter b is the strain hardening ratio. The curvature of the transition curve between the two asymptotes is governed by the parameter R (Fig. 6(b)), which permits the Bauschinger effect to be represented. The curvature parameter R depends on the absolute strain difference ξ between the current asymptotes' intersection point and the previous maximum or minimum strain reversal point (Fig. 6(b)). The parameter is assigned a value of R_0 for initial (or monotonic) loading, and the degradation of the curvature with each subsequent cycle is represented by experimentally determined parameters a_1 and a_2 as noted in Fig. 6(b).

Uniaxial concrete constitutive model

The hysteretic stress-strain relation of concrete for use in a MVLEM should address important issues such as the hysteretic behavior in both cyclic compression and tension, the progressive degradation of stiffness of both the unloading and reloading curves for increasing values of strain, and gradual crack closure. The uniaxial hysteretic constitutive model for concrete developed by Chang and Mander[10] is used as the basis for the material model implemented in this study. Details of the model are presented in the following paragraphs.

Chang and Mander[10] developed a generalized model to simulate the hysteretic behavior of confined and unconfined, ordinary, and high-strength concrete in both cyclic compression and tension, in which the monotonic curve forms the envelope for the cyclic stress-strain behavior. Particular emphasis was paid to the transition between crack opening and closure, and concrete in tension is modeled with a cyclic behavior similar to that in compression based on results of cyclic tension tests performed on concrete specimens by previous researchers. The model's envelopes for compression and tension allow

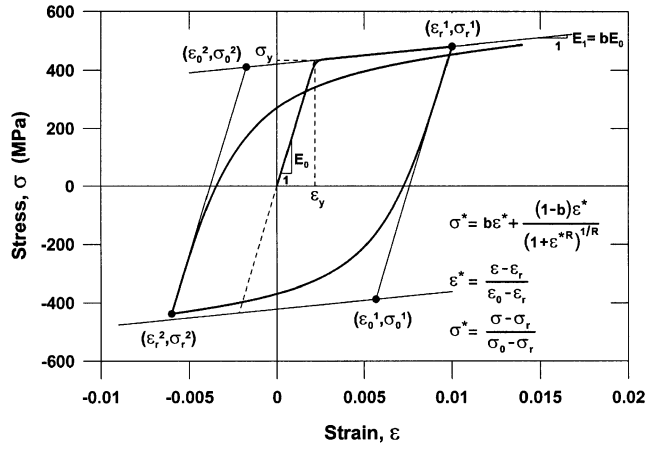

Note - ε_r, σ_r : strain and stress at reversal point
ε_0, σ_0 : strain and stress at intersection of the asymptotes

(a) Governing Equation

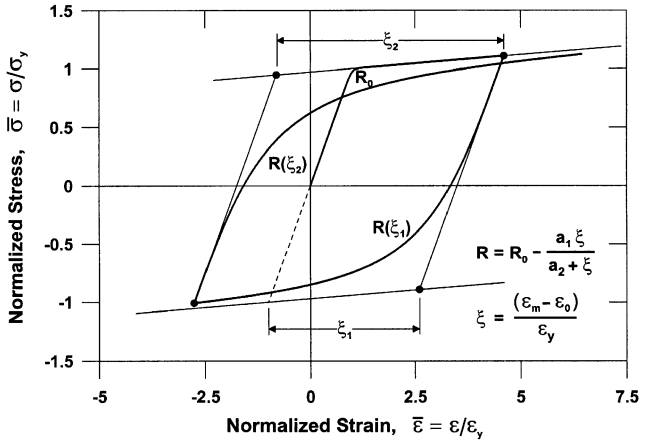

Note - ε_m : strain at reversal point (ε_r) for the previous cycle

(b) Degradation of Curvature

Fig. 6—Steel, uniaxial, cyclic, constitutive model.

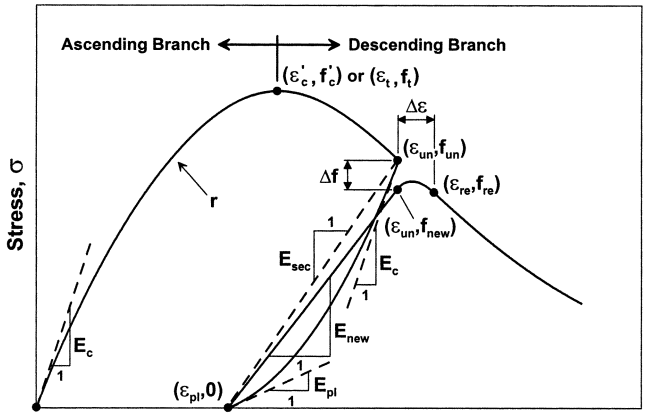

(a) Hysteretic Parameters

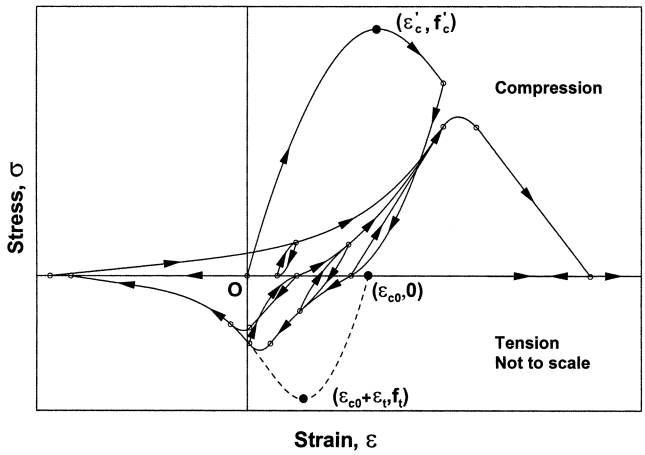

(b) Hysteresis in Compression and Tension

Fig. 7—Concrete, uniaxial, cyclic constitutive model (Chang and Mander[10]).

control on the shape of both the ascending and descending (that is, prepeak and postpeak) branches of the stress-strain behavior (Fig. 7(a)). The envelopes can be calibrated for selected values of peak stress, strain at peak stress and modulus of elasticity (and also via the parameter *r* defining the shape of the envelope curve), allowing for model refinement.

To define the cyclic properties of concrete in compression, statistical regression analyses were performed by Chang and Mander on an extensive experimental database and empirical relations were developed for key hysteretic parameters such as secant stiffness E_{sec} and plastic stiffness E_{pl} upon unloading from, and stress and strain offsets (Δf and $\Delta\varepsilon$) upon return to, the compression envelope (Fig. 7(a)). For cyclic behavior in tension, Chang and Mander modified the empirical relations for the same parameters used for compression, based on test results by Yankelevsky and Reinhardt.[11] Parameters such as the plastic (residual) strain upon unloading ε_{pl}, new stress f_{new}, and slope E_{new} upon returning to unloading strain ε_{un}, and the strain ε_{re}, stress f_{re}, and slope E_{re} upon returning to the compression or tension envelope are dependent on these empirical relations (Fig. 7(a)).

In terms of hysteretic behavior, the model uses smooth connecting curves for unloading and reloading between the compression and tension envelopes, and smooth transition curves for partial unloading and reloading between the connecting curves (Fig. 7(b)). Both connecting and transition curves have slope continuity with a constant sign of curvature (second derivative of the curve equation). Accordingly, the model generates a continuous stress-strain relation with slope continuity (except at unloading points) for confined and unconfined concrete in both compression and tension (Fig. 7(b)). Further details of the model can be found in the referenced report.[10] The model was verified by Chang and Mander for cyclic compression using an extensive test database and was shown to accurately simulate test results for both confined and unconfined concrete.

Modeling of tension stiffening

The contribution of tensile concrete resistance between cracks is known as tension stiffening and plays a significant role in reducing the postcracking deformations of reinforced concrete structures.[12] According to Belarbi and Hsu,[12] modeling of the tension stiffening phenomenon must consider two effects simultaneously. First, an average tensile stress-strain curve must be considered for cracked concrete; and second, the stress-strain curve of bare mild steel bars must be replaced by an average stress-strain curve for steel bars stiffened by concrete between cracks.

In this study, concrete and steel within each uniaxial element are subjected to the same average (smeared) strain. This allows direct implementation of average stress-strain

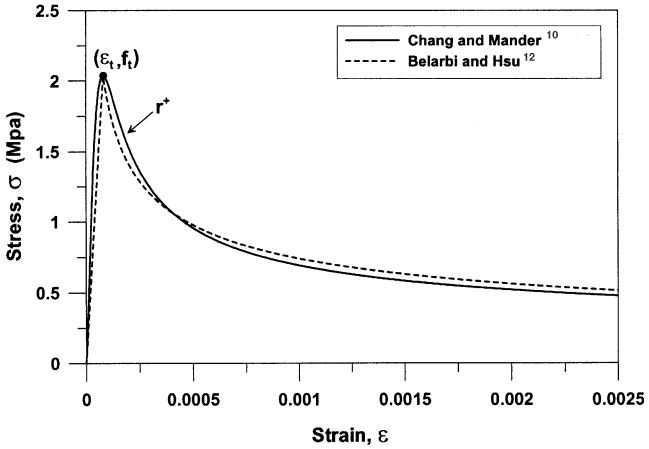

Fig. 8—Stress-strain envelopes for concrete in tension.

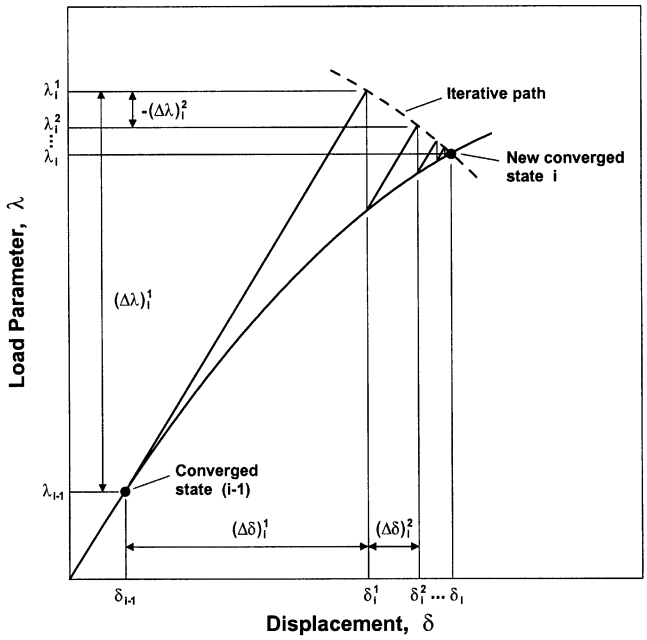

Fig. 9—Nonlinear analysis solution strategy.

relationships to assess the effect of tension stiffening on both steel and concrete. Belarbi and Hsu[12] developed a constitutive law for the average tensile stress-strain relationship of concrete in the monotonic postcrack region and proposed empirical modification factors, based on longitudinal steel area ratios, for the yield stress σ_y and strain-hardening ratio b of steel bars embedded in concrete.

The material laws implemented in this study can be controlled and calibrated to follow the relations developed by Belarbi and Hsu[12] or similar empirical relations to model tension stiffening for monotonic loading. The calibrated material laws can be used for cyclic loading, as a tension envelope for concrete or a tensile yield asymptote for steel, assuming that tension stiffening does not significantly influence the cyclic stress-strain properties of the materials. For example, Fig. 8 shows a comparison of a sample tension envelope generated by the model of Chang and Mander[10] with the descending branch of the stress-strain relationship proposed by Belarbi and Hsu.[12] The shape of the tension envelope in Chang and Mander's model is controlled through the parameter r for tension (in addition to the

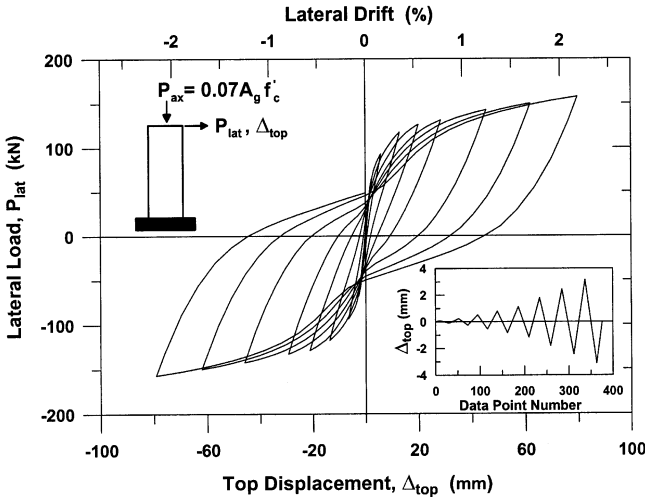

Fig. 10—Load-displacement response predicted by MVLEM.

modulus of elasticity E_c, the peak tensile stress f_t, and the strain at peak tensile stress ε_t). The primary difference in the two tension envelopes is that the envelope generated using the Chang and Mander model accounts for the nonlinearity of the stress-strain relation prior to cracking.

NONLINEAR ANALYSIS SOLUTION STRATEGY

The aforementioned macro wall model was implemented in Matlab[13] together with a direct stiffness assembly procedure to assemble the MVLEM elements into a complete wall model and an incremental-iterative numerical scheme to perform nonlinear quasistatic (monotonic or cyclic) analysis of the wall model. A displacement-controlled iterative solution strategy based on a specified incrementation of a selected displacement component (DOF) was adopted in this study. Iterations are performed on both displacement and load components (Fig. 9) to obtain static equilibrium within a specified tolerance, while keeping the value of the selected displacement component constant. Details of this iterative strategy are presented in the paper by Clarke and Hancock.[14] This solution strategy was selected to better correlate the model response with drift-controlled cyclic test results on RC wall specimens[15,16] subjected to prescribed lateral displacement histories at the top of the wall. Various incremental-iterative solution strategies can be implemented for the nonlinear analysis of the wall model depending on the type of loading. For example, the force-controlled Newton-Raphson solution scheme was implemented as part of the solution strategy for nonlinear dynamic analysis of the wall model.

ANALYSIS RESULTS AND PARAMETRIC SENSITIVITY STUDIES

The wall specimens tested by Thomsen and Wallace[15] and Taylor, Cote, and Wallace[16] are being used to assess and calibrate the aforementioned model. Design and reinforcement details for the walls, as well as the loading protocol, are presented in detail in the referenced report[15]/paper.[16] Details of the model calibration and comparison of the analytical and experimental results will be presented in a future publication. This paper focuses on characteristic features of the model as well as the sensitivity of the model response to changes in model parameters and material constitutive laws. Figure 10 shows a sample lateral load-top displacement response prediction for a rectangular wall specimen (Specimen RW2

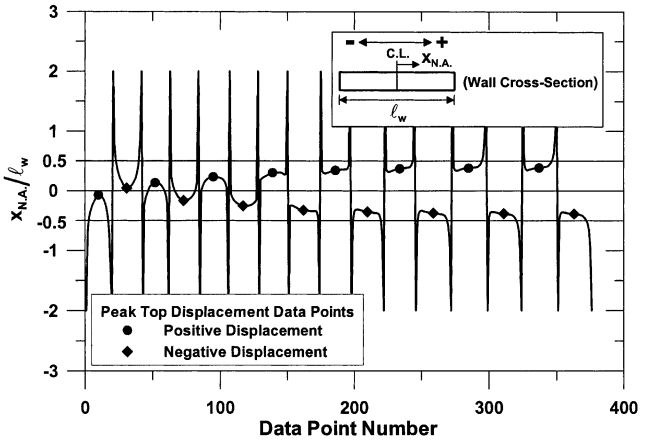

Fig. 11—Predicted variation in position of neutral axis.

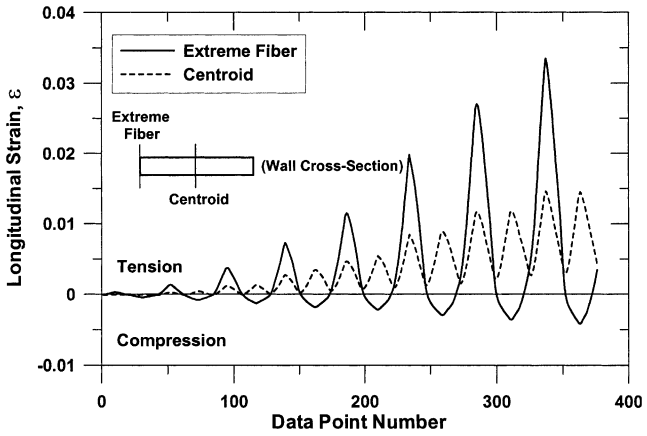

Fig. 12—Predicted longitudinal strain histories.

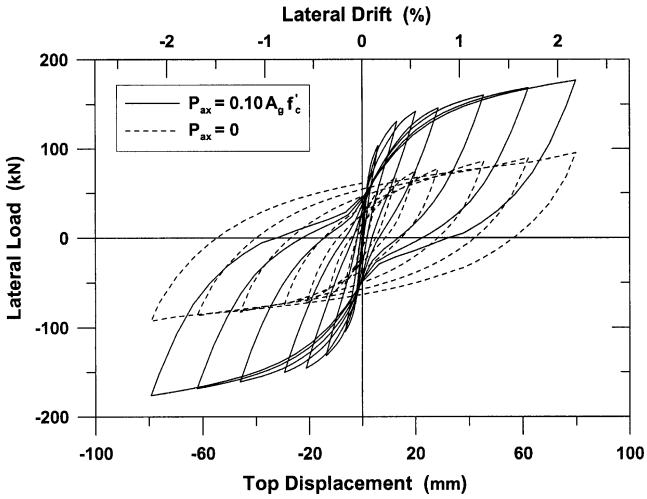

Fig. 13—Effect of axial load on analytical response.

tested by Thomsen and Wallace[15]) with height of 3.66 m, thickness of 102 mm, length of 1.22 m, and an applied axial load of approximately 7% of the axial load capacity of the specimen. The analytical results were obtained using eight MVLEM elements along the height of the wall, eight uniaxial elements (macrofibers) along the length, and $c = 0.4$ for an applied lateral displacement history at the top of the wall similar to the one used in the test program (cyclic drift levels of 0.1, 0.25, 0.5, 0.75, 1, 1.5, 2, and 2.5%). The applied lateral displacement history was corrected for the pedestal rotation of the wall specimen. The analysis results clearly reflect actual characteristics of cyclic wall behavior, including stiffness degradation, shape of the load-displacement hysteresis loops, plastic (residual) displacements at zero load, and pinching. The model successfully allows variation of the neutral axis depth for a cyclic displacement history applied at the top of the wall, as shown in Fig. 11, which displays the predicted position of the neutral axis in the MVLEM at the base of the wall, normalized by the wall length. The distance from the centroid of the wall cross section to the neutral axis approaches infinity when the lateral displacement (and thus rotation) of the wall approaches zero and reaches its local extrema or limit points (peaks and valleys) at peak displacement (displacement reversal) points. Figure 12 compares the average longitudinal strain histories predicted at the extreme concrete fiber and at the centroid of the wall for the element at the base of the wall, demonstrating the effect of applied displacement history and neutral axis migration on the predicted strains. The longitudinal strains are not symmetric with respect to the zero strain axis, and the strains predicted at the centroid are tensile for almost the entire loading history, except for a range of small displacements (due to the presence of axial load). Furthermore, the MVLEM directly considers the effect of varying axial load on the wall response, which although constant in this case, might vary in some cases (for example, under dynamic loads such as earthquakes). Figure 13 shows a comparison of the analytically predicted lateral load versus top displacement responses for an applied axial load of zero and 10% of the axial load capacity of the wall, clearly displaying the significant impact of axial load on the wall response.

In addition to the model parameters (number of macro wall elements m, number of uniaxial elements or macrofibers within each element n, and center of rotation parameter c), properties of the uniaxial hysteretic models defined for the materials influence the analytical response predictions. The sensitivity of the results obtained with the model to both model and material parameters is addressed in the following sections.

Material parameters

The MVLEM implemented in this study relates the predicted flexural response directly to material behavior without incorporating any additional empirical relations, as has been done in other studies.[1,7] It has been observed that the predicted load-displacement response is, as expected, influenced by the properties of the stress-strain laws assumed for the longitudinal reinforcement and the concrete; therefore, it is necessary to understand how variations in the material constitutive laws influence the results obtained using the model, particularly in the context of performance-based seismic design.

The material constitutive parameters associated with the implemented steel stress-strain law are the modulus of elasticity E_0, the yield stress σ_y, the strain-hardening ratio b, and the parameters R_0, a_1, and a_2 influencing the cyclic curvature of the transition curve between the elastic and yield asymptotes. Values for E_0, σ_y, and b are obtained from monotonic stress-strain tests conducted on bare reinforcing bar specimens, allowing for a reliable calibration. The values for the yield stress σ_y and strain-hardening ratio b, however, should be modified to consider the tension stiffening effect on the reinforcing bars and can be calibrated for average values

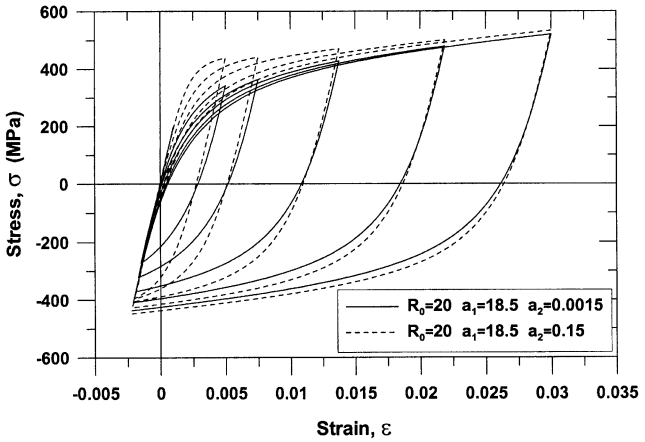

(a) Steel Stress-Strain Response Histories

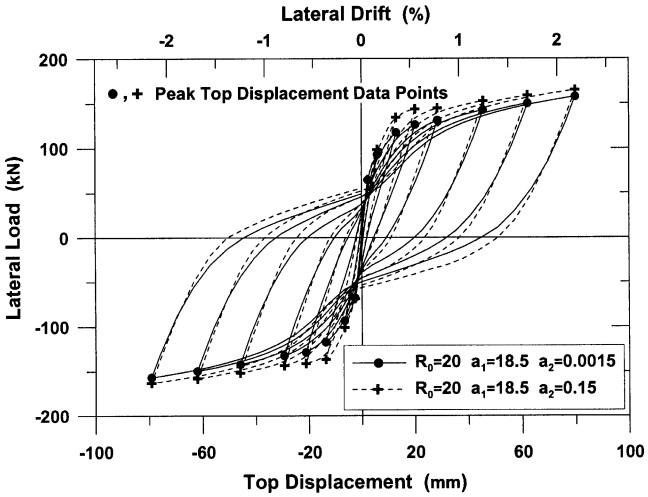

(b) Load-Displacement Response

Fig. 14—Sensitivity of analytical response to steel stress-strain parameters.

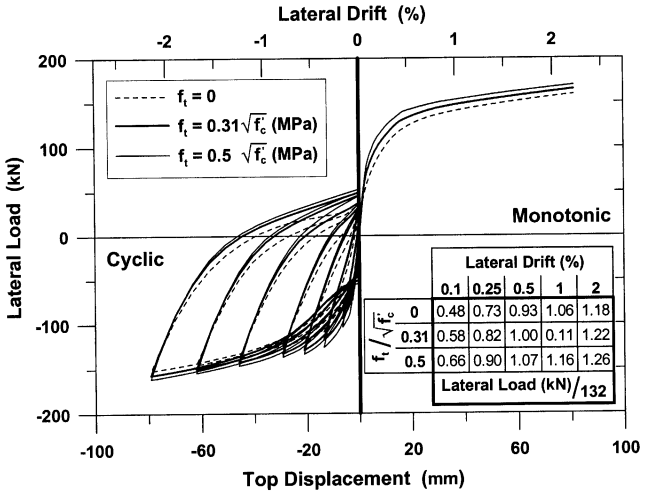

Fig. 15—Effect of concrete tensile strength on analytical response.

using relations such as those proposed by Belarbi and Hsu.[12] The calibration of parameters R_0, a_1, and a_2 (accounting for the cyclic degradation of the curvature coefficient R) requires cyclic test results, the availability of which is relatively limited. Figure 14(a) shows arbitrary stress-strain histories generated by the steel constitutive model for two different sets of values for parameters R_0, a_1, and a_2 calibrated by prior researchers[9,17] based on cyclic test results on steel bars. The analytically predicted lateral load-top displacement responses of the wall specimen obtained from the MVLEM using the specified values for the material parameters (R_0, a_1, and a_2) are shown in Fig. 14(b). The lateral load capacity of the wall is significantly influenced by these hysteretic parameters, primarily in the region where the steel is not subjected to high postyield strains (for example, 0.5 to 0.75% drift). Cyclic degradation of the lateral stiffness during unloading and plastic (residual) displacements at zero lateral load also depend on the selection of these parameters (Fig. 14(b)).

The material parameters associated with the implemented concrete stress-strain law are the monotonic (envelope) parameters (E_c, f_c' or f_t, ε_c' or ε_t, r) and the hysteretic parameters (Δf, $\Delta\varepsilon$, E_{pl}, E_{sec}) defined for compression and tension (Fig. 7(a)). The empirical relations used to define these parameters for monotonic and cyclic compression (for both confined and unconfined concrete) were validated by Chang and Mander[10] using extensive experimental data. The relations defining the parameters for cyclic tension, however, were obtained using limited experimental data. Furthermore, the observed tensile strength and stress-strain properties of concrete depend strongly on the testing conditions[10] and considerable data scattering is observed in test results, making it difficult to assign values for the parameters that define the concrete tensile stress-strain relation. Therefore, the sensitivity of the predicted wall response to concrete stress-strain parameters investigated herein focuses on concrete tensile strength and the hysteretic parameters related to cyclic tension, as well as because model results are less sensitive to variations in the parameters describing the behavior of concrete in compression. Figure 15 illustrates how the predicted monotonic and cyclic lateral load-top displacement responses of the wall specimen (with applied axial load 7% of axial load capacity) are influenced by selection of the tensile strength (peak tensile stress) for concrete f_t. The strain at peak tensile stress ε_t was varied proportionally with the peak tensile stress while the shape parameter r was kept constant. Neglecting the contribution of concrete in tension results in a lower prediction of the wall lateral stiffness and a slightly lower prediction of the wall lateral strength compared with results that include the contribution of concrete in tension. Furthermore, variation in the assumed tensile strength for concrete influences the cyclic properties of the predicted response (Fig. 15).

The hysteretic parameters associated with the cyclic concrete stress-strain law in tension are the plastic stiffness E^+_{pl} and secant stiffness E^+_{sec} upon unloading from, and stress and strain offsets (Δf^+ and $\Delta\varepsilon^+$) upon return to the tension envelope (Fig. 7(a)). The predicted wall response is not notably influenced by the stress and strain offsets because the offsets influence the shape of the stress-strain curve within a very small range of tensile stresses. On the other hand, the predicted wall response is significantly influenced by values selected for the plastic and secant stiffnesses for unloading in tension because these parameters control the starting strain and initial slope for the gap closure region of the concrete stress-strain law. Figure 16(a) compares sample stress-strain histories generated by the constitutive relationship for concrete with the original expression derived by Chang and Mander[10] for the plastic

stiffness in tension E^+_{pl} and an illustrative value of zero, and Fig. 16(b) compares the corresponding predicted load-displacement responses of the wall obtained using 17 MVLEM elements along the wall height (eight of the MVLEM elements stacked along the bottom 1/4 of the wall height and the rest distributed uniformly over the wall height) with 22 uniaxial elements along the wall length, and $c = 0.4$. The figures reveal that the shape of the unloading and reloading curves of the predicted load-displacement response is governed by the selection of the value for plastic stiffness E^+_{pl}, which together with the secant stiffness E^+_{sec} governs the progressive gap closure properties (that is, pinching) of the concrete stress-strain relationship. Using a value of zero for E^+_{pl} results in an abrupt change in the lateral stiffness of the wall from unloading to reloading in the opposite direction, and thus a much more pronounced pinching behavior (similar to the cyclic response in Fig. 15, when concrete tensile stresses are neglected [$f_t = 0$] and thus the plastic stiffness for unloading in tension is zero), whereas implementing the original relation imposes a more gradual change in the lateral stiffness of the wall. The variation in the pinching behavior, however, does not change the lateral strength and stiffness of the wall at peak top displacement (displacement reversal) points because the enforced peak displacements of the wall are increasing for successive loading cycles.

Similar behavior is observed in the analytically predicted position of the neutral axis and the predicted longitudinal strains. Figure 16(c) shows the position of the neutral axis predicted in the MVLEM at the base of the wall obtained by using the two different expressions for the tensile plastic stiffness. The neutral axis positions reach the same local limit values at peak displacement data points, and variation between the two cases is enhanced as the displacement (or rotation) of the wall approaches zero. Finally, Fig. 16(d) illustrates the influence of the plastic stiffness on predicted longitudinal strain histories for the element at the base of the wall. For the two cases, the strains at both the extreme fiber and centroid are identical at peak displacement data points; however, noticeable variation is observed in the strains (more distinctly at the centroid) as the wall displacement approaches zero.

The variation in the unloading and reloading regions of the predicted response (Fig. 16(b)) has only a marginal effect on the energy dissipation capacity of the wall model. Calculating the hysteretic energy dissipation capacity for the plots in Fig. 16(b) normalized by that of a bilinear lateral load-top displacement relationship yields values of 0.66 for the response obtained by using the relation for the tensile plastic stiffness defined by Chang and Mander, and 0.64 using a zero value for the tensile plastic stiffness.

Variation in the secant stiffness defined for concrete in tension E^+_{sec} influences wall response in roughly the same way as changes in the plastic stiffness E^+_{pl}. The empirical relations defined by Chang and Mander for the plastic stiffness and secant stiffness in tension were obtained from limited experimental data[12] with imposed tensile strains reaching a value of approximately 0.003. However, the tensile strains in walls are likely to reach much larger values (for example, 0.035 in this example); thus, using the Chang and Mander empirical relations for such high levels of tensile strain may be inappropriate. Calibration of these two hysteretic parameters for a broader range of tensile strains, and also accounting for the tension stiffening effect, would

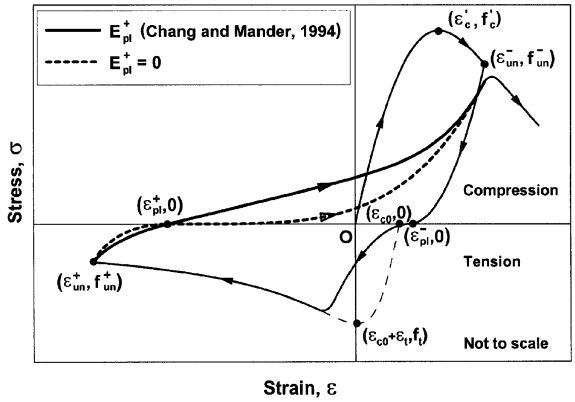

(a) Concrete Stress-Strain Relation

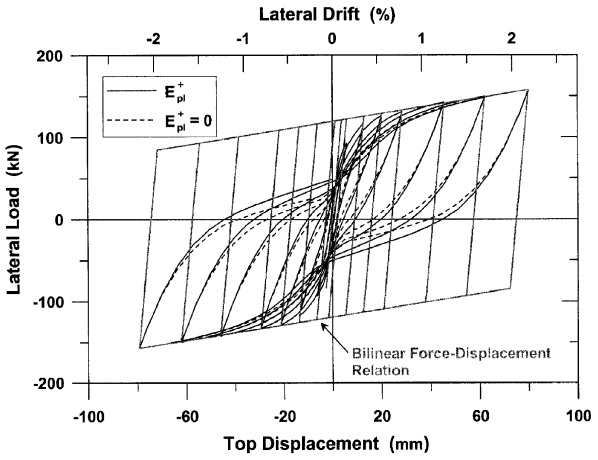

(b) Load-Displacement Response

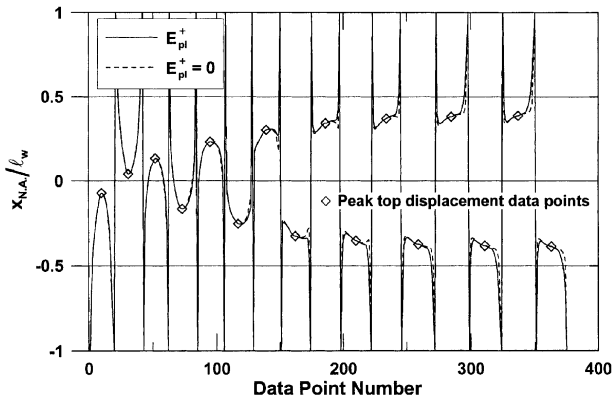

(c) Position of the Neutral Axis

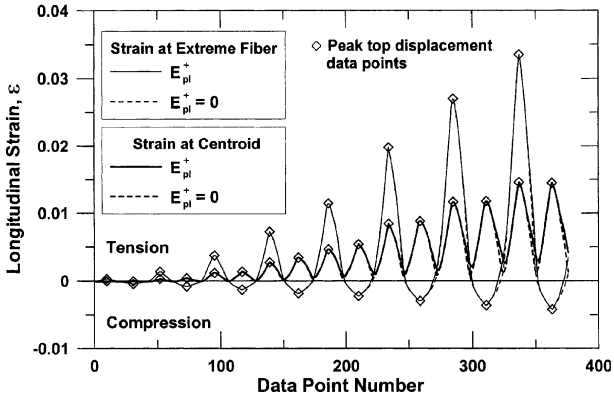

(d) Longitudinal Strains

Fig. 16—Effect of concrete tensile plastic stiffness on analytical response.

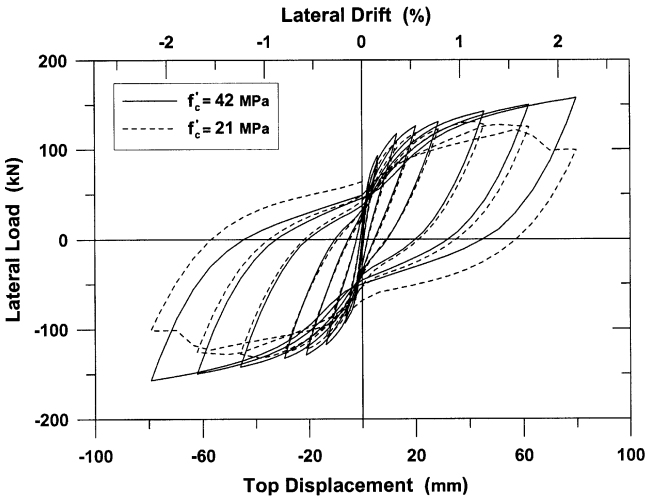

Fig. 17—Strength degradation in analytical response.

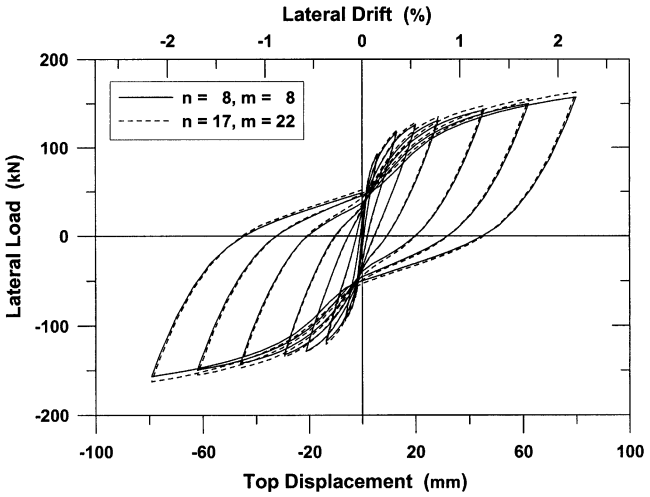

(a) Lateral Load – Top Displacement Response

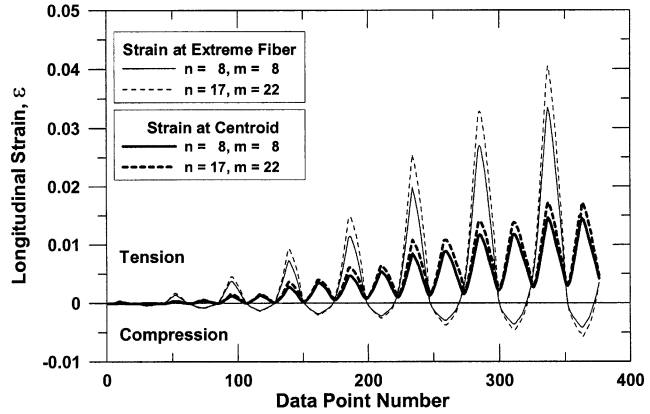

(b) Longitudinal Strains in the MVLE at the Base of the Wall

Fig. 18—Sensitivity of responses to number of MVLEM and uniaxial elements.

refine the modeling of the gap closure region of the concrete stress-strain behavior, and the prediction of the wall pinching behavior. The concrete model proposed by Chang and Mander[10] provides a flexible approach that allows calibration of such parameters to control gap closure properties of concrete for an improved overall representation of wall force-deformation relations.

It has been observed that the model results are less sensitive to variation in the parameters defining the monotonic and hysteretic stress-strain relation for concrete in compression, provided that the values used for the parameters are within reasonable range such as those obtained by using the empirical relations recommended by Chang and Mander. The empirical relations relate the parameters for compression (that is, modulus of elasticity E_c, strain at peak compressive stress ε_c', parameter r defining the shape of the compression envelope, and hysteretic parameters for compression including stress and strain offsets [Δf^- and $\Delta\varepsilon^-$], and unloading plastic stiffness and secant stiffness [E_{pl}^- and E_{sec}^-]) to the value selected for the unconfined compressive strength (peak unconfined compressive stress f_c') of ordinary or high-strength concrete. The governing parameter f_c' can be feasibly calibrated with monotonic stress-strain tests conducted on concrete specimens (for example, 152.5 x 305 mm standard cylinders). The macro wall model presented previously, together with the nonlinear solution strategy implemented here, can simulate the strength degradation associated with the descending (postpeak) branch of the concrete stress-strain constitutive law. This is shown in Fig. 17, where the analytical lateral load-top displacement responses obtained using different values of unconfined compressive strength are also compared.

Model parameters

Apart from material constitutive parameters, the only parameters associated with the analytical wall model are the number of uniaxial elements used along the length of the wall cross section n, the number of MVLEM elements stacked on top of each other along the height of the wall m, and the parameter defining the location of the center of rotation along the height of each MVLEM element c (Fig. 2). Sensitivity of the simulated wall response to variations of these parameters was investigated.

It has been observed that the calculated global response (that is, lateral load versus top-displacement) is not very sensitive to the selection of either the number of MVLEM elements along the height of the wall or the number of vertical elements along the wall length, provided that reasonable values are selected to adequately represent the overall wall geometry. Figure 18(a) shows a comparison of the lateral load-top displacement response predicted by using either eight MVLEM elements along the wall height with eight uniaxial elements along the length of the wall, or by using 17 MVLEM elements along the wall height (eight of the MVLEM elements stacked along the bottom 1/4 of the height where the inelastic deformations are expected, and the rest distributed uniformly over the wall height) with 22 uniaxial elements along the wall length. The comparison indicates that increasing the number of vertical line elements or the number of MVLEM elements does not change significantly the prediction of the global response (that is, lateral load versus top displacement); however, the use of more elements is valuable in terms of obtaining more detailed information on local behavior, such as the state of stress and strain or moment curvature response at a given location. For example, results shown in Fig. 18(b) compare the average longitudinal strain histories predicted at the extreme concrete fiber and the centroid of the wall, in the MVLEM at the base of the two wall model configurations

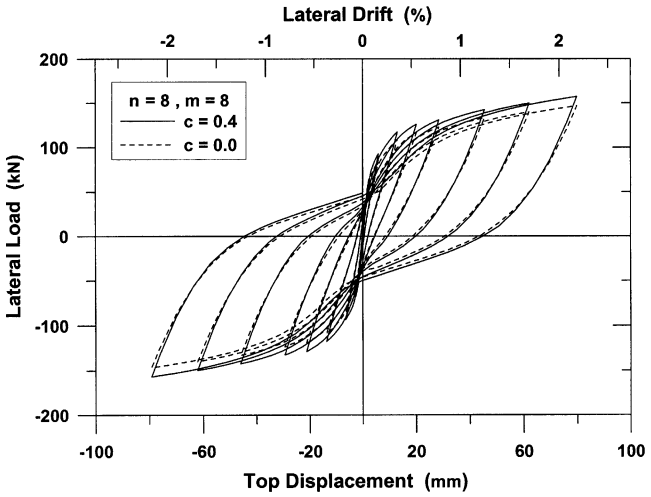

(a) Model with 8 MVLEM Elements and 8 Uniaxial Elements

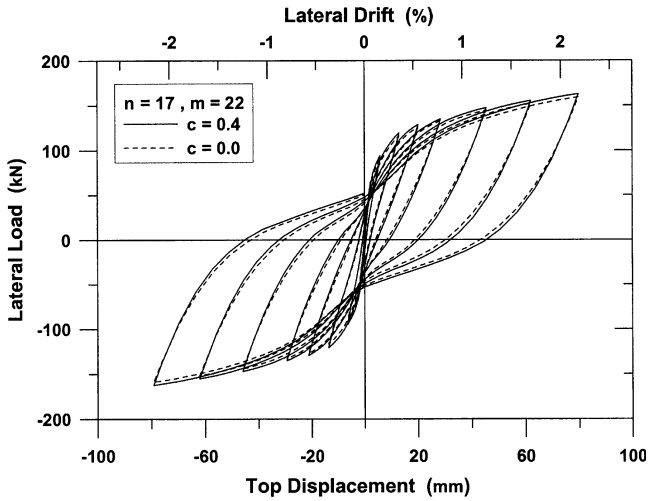

(b) Model with 17 MVLEM Elements and 22 Uniaxial Elements

Fig. 19—Sensitivity of response to parameter c.

used for the plots in Fig. 18(a) ($n = 8$, $m = 8$, and $n = 17$, $m = 22$). Using more MVLEs over the height of the wall allows for an improved local prediction of the strains. Also, using more uniaxial elements along the wall length allows for a more refined description of the wall cross section. Therefore, the model incorporates the flexibility to choose how much detail is desired in the analytical results.

The sensitivity of analysis results to the parameter defining the location of the center of rotation along the height of each MVLEM element c is illustrated in Fig. 19. Figure 19(a) compares the predicted lateral load-top displacement (global) response by using a wall model with eight MVLEM elements (and eight uniaxial elements) for a value of $c = 0.4$ (recommended by Vulcano, Bertero, and Colotti[1]) and an illustrative extreme value of $c = 0.0$ (center of rotation at the bottom of each MVLEM element). Decreasing the value of parameter c leads to a higher prediction of rotations and transverse displacements of the wall, resulting in a slightly lower prediction of the wall strength and lateral stiffness. This extreme variation in parameter c, however, does not influence the characteristic shape of the load-displacement response significantly. As proposed by Fischinger et al.[2], stacking more wall elements along wall height, especially in the region where inelastic deformations are expected, reduces the change in curvature within each element, thus diminishing the influence of the parameter c on the response. Figure 19(b) compares the predicted global wall response for $c = 0.4$ and $c = 0.0$ using a wall model with 17 MVLEM elements with eight of the elements stacked along the bottom 1/4 of the wall height. The two responses are very similar.

CONCLUSIONS

Use of an MVLEM provides an effective means to model the flexural response of slender reinforced concrete structural walls at both the global and local levels. The intent of this paper was to implement state-of-the-art, reliable, robust material constitutive laws into an MVLEM and demonstrate the effectiveness of the MVLEM for modeling and simulating the inelastic response of reinforced concrete structural walls. The variation of model and material parameters was investigated to identify the sensitivity of analytically predicted global and local wall responses to changes in these parameters as well as to identify which parameters require the greatest care with respect to calibration.

Based on analysis results, it was verified that the MVLEM captures important response characteristics associated with cyclic behavior of slender reinforced concrete structural walls governed by flexure. The analytical model is able to simulate important behavioral features including shifting of the neutral axis along the wall cross section and the effect of fluctuating axial force, which are commonly ignored in simple models. Characteristics of the cyclic response, including stiffness degradation and strength deterioration, hysteretic shape, and pinching behavior are clearly captured in the analysis results.

The modeling approach adopted here involves implementing refined hysteretic uniaxial stress-strain laws instead of simplified (ad-hoc) force-deformation rules to track nonlinear responses. This allows the designer to relate analytical responses directly to physical material behavior and provides a more robust modeling approach, where model improvements result from improvement in constitutive models and refinement in the spatial resolution of the discrete model. For concrete, the advanced constitutive models proposed by Chang and Mander[10] were implemented because they allow control on the monotonic and hysteretic parameters for an improved representation of the material stress-strain behavior. This provides a direct and flexible approach to incorporate important material behavioral features (for example, hysteretic behavior in tension, progressive gap closure, tension stiffening effect) into the analysis. It has been observed that the model responses are not only sensitive to material parameters associated with the monotonic stress-strain behavior, but also influenced significantly by variation in the hysteretic parameters defined for the steel (R_0, a_1, a_2) and for concrete in tension (E^+_{pl}, E^+_{sec}). Thus, careful calibration of these parameters is important for an improved prediction of the cyclic wall response.

Overall, the macroscopic wall model presented herein provides a flexible platform to assess the influence of various material and behavioral features in the nonlinear responses of slender RC structural walls. Calibration of the model using experimental results and implementation of the model into a computational platform (for example, Pacific Earthquake Engineering Research Center[18]) will provide design engineers improved analytical capabilities to model the behavior of structural walls and their interaction with

other structural elements. This capability is important given the trend toward performance-based seismic design.

Details on calibration of the model and correlation of predicted local and global responses with extensive test results will be presented in a follow-up paper. Possible further model improvements include implementing axial force-deformation models in the uniaxial elements for modeling reinforcing bar buckling and bond slip. Additional work will focus on modeling of walls with flanged sections, modeling of the shear response, as well as modeling the coupling of shear and flexural behavior.

ACKNOWLEDGMENTS

The work presented in this paper was supported by funds from the National Science Foundation under Grant Nos. CMS-9632457 and CMS-9810012. Opinions, findings, conclusions, and recommendations in this paper are those of the authors and do not necessarily represent those of the sponsor.

REFERENCES

1. Vulcano, A.; Bertero; V. V.; and Colotti, V., "Analytical Modeling of RC Structural Walls," *Proceedings*, 9th World Conference on Earthquake Engineering, V. 6, Tokyo-Kyoto, Japan, 1988, pp. 41-46.

2. Fischinger, M.; Vidic, T.; Selih, J.; Fajfar, P.; Zhang, H. Y.; and Damjanic, F. B., "Validation of a Macroscopic Model for Cyclic Response Prediction of RC Walls," *Computer-Aided Analysis and Design of Concrete Structures*, V. 2, N. B. Bicanic and H. Mang, eds., Pineridge Press, Swansea, Wales, 1990, pp. 1131-1142.

3. Fischinger, M.; Vidic, T.; and Fajfar, P., "Nonlinear Seismic Analysis of Structural Walls Using the Multiple-Vertical-Line-Element Model," *Nonlinear Seismic Analysis of RC Buildings*, H. Krawinkler and P. Fajfar, eds., Elsevier Science Publishers Ltd., London and New York, 1992, pp. 191-202.

4. Kabeyasawa, T.; Shiohara, H.; Otani, S.; and Aoyama, H., "Analysis of the Full-Scale Seven-Story Reinforced Concrete Test Structure," *Journal of the Faculty of Engineering*, University of Tokyo (B), Tokyo, Japan, V. 37, No. 2, 1983, pp. 431-478.

5. Vulcano, A., and Bertero, V. V., "Analytical Models for Predicting the Lateral Response of RC Shear Walls: Evaluation of Their Reliability," *EERC Report* No. UCB/EERC-87/19, Earthquake Engineering Research Center, University of California, Berkeley, Calif., 1987, 99 pp.

6. Vulcano, A., "Macroscopic Modeling for Nonlinear Analysis of RC Structural Walls," *Nonlinear Seismic Analysis of RC Buildings*," H. Krawinkler and P. Fajfar, eds., Elsevier Science Publishers Ltd., London and New York, 1992, pp.181-190.

7. Colotti, V., "Shear Behavior of RC Structural Walls," *Journal of Structural Engineering*, ASCE, V. 119, No. 3, 1993, pp. 728-746.

8. Menegotto, M., and Pinto, E., "Method of Analysis for Cyclically Loaded Reinforced Concrete Plane Frames Including Changes in Geometry and Non-Elastic Behavior of Elements Under Combined Normal Force and Bending," *Proceedings*, IABSE Symposium on Resistance and Ultimate Deformability of Structures Acted on by Well-Defined Repeated Loads, Lisbon, Portugal, 1973, pp. 15-22.

9. Filippou, F. C.; Popov E. G.; and Bertero, V. V., "Effects of Bond Deterioration on Hysteretic Behavior of Reinforced Concrete Joints," *EERC Report* No. UCB/EERC-83/19, Earthquake Engineering Research Center, University of California, Berkeley, Calif., 1983, 184 pp.

10. Chang, G. A., and Mander, J. B., "Seismic Energy Based Fatigue Damage Analysis of Bridge Columns: Part I—Evaluation of Seismic Capacity," *NCEER Technical Report* No. NCEER-94-0006, State University of New York, Buffalo, N.Y., 1994, 222 pp.

11. Yankelevsky, D. Z., and Reinhardt, H. W., "Response of Plain Concrete to Cyclic Tension," *ACI Materials Journal*, V. 84, No. 5, Sept.-Oct. 1987, pp. 365-373.

12. Belarbi, H., and Hsu, T. C. C., "Constitutive Laws of Concrete in Tension and Reinforcing Bars Stiffened by Concrete," *ACI Structural Journal*, V. 91, No. 4, July-Aug. 1994, pp. 465-474.

13. The Math-Works, Inc., "Matlab," Natick, Mass., 2001.

14. Clarke, M. J., and Hancock, G. J., "A Study of Incremental-Iterative Strategies for Non-Linear Analyses," *International Journal for Numerical Methods in Engineering*, V. 29, 1990, pp. 1365-1391.

15. Thomsen, J. H., and Wallace, J. W., "Displacement-Based Design of RC Structural Walls: An Experimental Investigation of Walls with Rectangular and T-Shaped Cross-Sections," *Report* No. CU/CEE-95/06, Department of Civil Engineering, Clarkson University, Postdam, N.Y., 1995, 353 pp.

16. Taylor, C. P.; Cote, P. A.; and Wallace, J. W., "Design of Slender RC Walls with Openings," *ACI Structural Journal*, V. 95, No. 4, July-Aug. 1998, pp. 420-433.

17. Elmorsi, M.; Kianush, M. R.; and Tso, W. K., "Nonlinear Analysis of Cyclically Loaded Reinforced Concrete Structures, *ACI Structural Journal*, V. 95, No. 6, Nov.-Dec. 1998, pp. 725-739.

18. Pacific Earthquake Engineering Research Center, "OpenSees—Open System for Earthquake Engineering Simulation," http://opensees.berkeley.edu/OpenSees/developer.html.